Boundary Layer Meteorology manuscript No. 335

Large Aperture Scintillometer Intercomparison Study

J. Kleissl, J. Gomez, S.-H. Hong, J.M.H.

Hendrickx, T. Rahn, W.L. Defoor

Received: August 7, 2007 / Accepted: date

Abstract Two field studies with six large aperture scintillometers (LASs) were performed using horizontal and slant paths. The accuracy of this novel and increasingly popular technique for measuring sensible heat fluxes was quantified by comparing measurements from different instruments over nearly identical transects. Random errors in LAS measurements were small, since correlation coefficients between adjacent measurements were greater than 0.995. However, for an ideal set-up differences in linear regression slopes of up to 21% were observed with typical inter-instrument differences of 6%. Differences of 10% are typical in more realistic measurement scenarios over homogeneous natural vegetation and different transect heights and locations. Inaccu-

J. Kleissl

Dept. of Mechanical and Aerospace Engineering, University of California, San Diego

Tel.: +1-443-527-2740

E-mail: jkleissl@ucsd.edu

J. Gomez · S.-H. Hong · J.M.H. Hendrickx · W.L. Defoor

Dept. of Earth and Environmental Sciences, New Mexico Tech, Socorro, NM

T. Rahn

Los Alamos National Lab, Los Alamos, NM

racies in the optics, which affect the effective aperture diameter, are the most likely explanation for the observed differences.

Keywords Large Aperture Scintillometer · Sensible Heat Flux · Instrument Intercomparison

1 Introduction

A major challenge for the validation of remote sensing algorithms that estimate the surface energy balance is the ground measurement of sensible heat fluxes at a scale similar to the spatial resolution of the remote sensing image. While the pixel size of thermal remote sensing images covers a range from 60 m (Landsat7), 1000 m (MODIS), to 4000 m (GOES) direct methods to measure sensible heat fluxes such as eddy covariance (EC) only provide point measurements with a footprint at a scale that can be considerably smaller than a satellite pixel (except for Landsat). Since the footprint area of a large aperture scintillometer (LAS) measurement is larger (up to 5000 m in one dimension) and its spatial extent better constrained than that of EC systems, LASs offer the unique possibility of measuring the vertical flux of sensible heat averaged over areas comparable to one or more pixels of a satellite image or mesoscale numerical weather model (Hemakumara et al. 2003; Schüttemeyer 2005; Hafeez et al. 2006; Hendrickx et al. 2007). A LAS receiver measures intensity fluctuations in the radiation I emitted by the transmitter at a distance of 500 - 5000 m to derive the structure parameter of temperature, C_T^2 [$\mathrm{K}^2\ \mathrm{m}^{-2/3}$]. Refractive scattering by density variations due to turbulent eddies along the propagation path causes these intensity fluctuations. From C_T^2, together with an estimate of the roughness length and wind speed measurements

at one height, the sensible heat flux can be calculated using Monin-Obukhov similarity theory (MOST).

Micrometeorological investigations have demonstrated that, as with EC systems, LASs can be used to estimate sensible heat fluxes in the atmospheric surface layer (Andreas 1990; Hill et al. 1992a,b; de Bruin 2002 and other articles in the 2002 special Boundary–Layer Meteorology issue on scintillometry). LASs have been successfully used in a wide variety of environments (e.g. de Bruin et al. 1995; Meijninger and de Bruin 2000; Schüttemeyer 2005) and have also been validated over heterogeneous landscapes against EC measurements (Beyrich et al. 2002; Meijninger et al. 2002).

A useful point of reference to this study is the uncertainty in flux measurements using EC systems, which have been used for several decades to measure turbulent heat fluxes in the atmospheric surface layer (e.g. Katul et al. 1999). An EC system typically consists of a three-dimensional (3D) sonic anemometer-thermometer (SAT) operated at 10 Hz or faster and a scalar sensor in close proximity (for sensible heat flux measurements this is often a fine wire thermocouple). The sensible heat flux H is then computed directly from covariances in the vertical velocity w and air temperature T as $H = \rho_{air} c_p \left\langle w'T' \right\rangle$, where ρ_{air} is the air density, c_p is the specific heat capacity at constant pressure, the brackets denote temporal averaging, and w' and T' are the differences between, respectively, the instantaneous vertical wind speed and air temperature and their averages over 10 to 30 minutes. However, several non-trivial corrections have to be applied to the measurements, and even then the sum of the sensible and latent turbulent fluxes from EC systems are typically 10-15% smaller than the available energy, i.e. the difference of net radiation (R_{net}) and soil heat flux, an issue known as energy balance non-closure that has yet to be resolved (e.g. Wilson et al. 2002; Foken et al. 2006).

EC flux measurement uncertainties have been examined in detail by Loescher et al. (2005) by comparing laboratory and field data of SATs from eight different manufacturers. Exercising great care in data collection and processing, they found uncertainties in $\langle w'T' \rangle$ among sensors due to their different responses to air temperature for each 15-min averaging period ranging from -23.1 to $+16.1\%$. They ranged from -1 to $+8\%$ when averaged over 940 periods and corrected for mean temperature offsets. Linear regressions for $\langle w'T' \rangle$ of seven instruments versus the eighth in neutral to unstable stability conditions revealed differences in slopes ranging from 19-31%, coefficients of variation typically greater than 95%, while standard deviations of the slopes (i.e. a typical measure of the slope for any two sensors) were between 7-11%. Errors in stable conditions were even larger but will not be examined herein.

Van der Molen et al. (2004) found that SAT vertical wind velocities were underestimated for large angles of attack (the vertical angle between the wind vector and a horizontal plane) and wind direction. By applying empirical sine corrections they found that scalar covariances were also underestimated by 5-15%. Gash and Dolman (2003) argued that winds with large angles of attack typically have a large covariance between vertical velocity and temperature. As a result underestimation of these velocities results in loss of a large percentage of the total turbulent flux.

Instrument intercomparison studies for LAS have not been carried out to date, because commercial manufacturing of LASs has only begun recently and they are still more expensive than SATs. However, LASs are quickly gaining wide acceptance (Poggio et al. 2000; Nakaya et al. 2007, Asanuma and Iemoto 2007) – e.g. 12 LASs are in operation in Texas, New Mexico (Hendrickx et al. 2007), and California, U.S.A. LASs would also be an integral part of proposed US hydrologic observatory efforts (John Wilson, New Mexico Tech, personal communication, 2007) and may present a

unique opportunity for data assimilation of surface fluxes into mesoscale meteorological models. Consequently, there is a clear need for establishing the accuracy of LASs.

Since LASs rely on MOST, the derived sensible heat flux can only be as accurate as the theory itself, which is mostly a concern in stable and free convective (Hill 1997) atmospheric conditions. Moreover, the LAS is only sensitive to inertial range eddy scales (Meijninger 2003). The method (Eq. 1 below) prescribes the inertial spectrum shape to determine C_n^2, thus ignoring non-turbulent contributions to the spectrum of the refractive index n, such as low frequency motions or non-stationary conditions. In addition, the LAS does not measure the friction velocity u_*. Thus additional measurements of wind speed, an estimate of roughness length, and flux profile relationships are required.

In this paper we do not attempt to examine the absolute accuracy of LAS sensible heat flux measurements: neither do we examine the validity of MOST nor is the true sensible heat flux (as measured by a non-existing perfect sensor) available for intercomparison. However, by comparing data from up to five adjacent LAS transects over homogeneous areas with natural vegetation we examined the robustness of the instrument and the scintillation technique. The paper focuses on ideal experiments with nearly identical transect lengths and beam heights, but we also briefly discuss results from experiments with larger transect spacings and slant paths. In Section 2 we will present the field experiments. Section 3 deals with the methods to derive sensible heat fluxes from LAS, and Section 4 shows the intercomparisons among LASs and between LAS and EC systems.

2 Field Experiments

2.1 General Considerations

Transmitter power and aperture of a large aperture scintillometer (LAS) are designed for transect distances (i.e. the distance between transmitter and receiver) of up to 5 km. The LAS has to be placed in the atmospheric surface layer, where Monin-Obukhov similarity theory applies. The LAS beam height and set-up distance have to be carefully chosen, such that the LAS operates in the weak scattering regime, where the structure parameter of the refractive index C_n^2 is small enough that it can be derived from the variance of signal intensity I from first-order scattering theory (Clifford et al. 1974) for given values of aperture diameter D and transect length L

$$C_n^2 = 1.12 D^{7/3} L^{-3} \sigma_{lnI}^2. \quad (1)$$

For strong scattering, an increase in C_n^2 no longer results in an increase in the variance of the natural log of signal intensity σ_{lnI}^2, i.e. the signal intensity variation is 'saturated' and Eq. 1 no longer holds. Since C_n^2 is proportional to $z^{-4/3}$ in unstable conditions, the requirement of weak scattering necessitates raising the LAS transect for longer distances and larger sensible heat fluxes. For example, for typical midday conditions at the Sevilleta, New Mexico, site (see below), where $H = 200$ W m^{-2} and $L = 2800$ m, the transect height should be greater than 17 m to remain in the weak scattering regime and avoid saturation of the signal (Meijninger 2003, Kohsiek et al. 2006).

For the present study, measurements were taken in the course of one set of experiments using horizontal beams (H1-H2) and one set of experiments using slant paths (S1-S4, Table 1). All LASs used in this study were new (purchased in 2005 and 2006)

Table 1 LAS experiments in chronological order, where date is given as day/month/year: S: slant path (Sevilleta NWR), H: horizontal path (Valles Caldera NP). In each cell the first value is the effective beam height [m] calculated for free convective conditions, and the second value is the distance [m] between receiver and transmitter.

	Experiment name and duration					
LAS Serial number	S1 27/11/2005- 2/12/2005	S2 2/12/2005- 13/12/2005	S3 16/12/2005- 18/1/2006	S4 18/1/2006- 8/2/2006	H1 6/6/2006- 20/6/2006	H2 20/6/2006- 29/6/2006
$^{0300}05$	19.1 1368	same as S1	datalogger malfunction		43.9 2014	same as H1
$^{0500}15$	23.9 1454	20.0 1365	20.0 2836	21.4 2751	43.5 2019	44.1 2009
$^{0500}16$	15.0 1266	17.3 1332	19.9 2675	19.8 2846	X	X
$^{0500}17$	17.5 1312	same as S1	18.7 2713	19.1 2810	44.1 2009	43.5 2019
$^{0600}31$	X	X	X	X	43.9 2013	43.1 2022
$^{0600}32$	X	X	X	X	43.1 2022	43.9 2013

and had not been deployed before. The only exception was LAS serial number $^{0300}05$ which was purchased in 2003 and deployed once in 2005. LAS $^{0300}05$ was sent to the factory for maintenance between experiment S4 and H1.

The goal of taking measurements over the same area had to be balanced with the fact that any two receivers on the same transect end have to be spaced laterally by at least $\approx 0.01L$ to avoid 'cross-contamination', since the transmitter beam spread is

$\approx 1\%$. Absence of cross-contamination of receiver signals was confirmed by switching off the corresponding transmitter during unstable conditions, which are subject to corresponding beam-widening, and observing the signal strength decrease to zero.

The LAS output wires for C_n^2 and signal strength voltage were connected to three CR10X, one CR1000 (via 1:1 voltage dividers), and one CR23X datalogger (all Campbell Scientific Inc.), sampled at 1 Hz and stored as 10-min averages. The LAS were set up on low, heavy, stable cinder blocks and iron tripods such that the influence of structural vibration on the measured intensity fluctuations can be ignored.

2.2 Horizontal Beams at the Valles Caldera National Preserve (VCNP)

Five Kipp and Zonen LAS were set up over a flat grassy highland (the Valle Grande) in the Valles Caldera National Preserve (VCNP), about 15 km west of Los Alamos, New Mexico from June 6 - June 29, 2006 (Fig. 1a, Table 1). Mean daily maximum and minimum air temperatures during the study were 23.6 ^oC and 4.4 ^oC, respectively, and only 1.5 mm of rain was recorded between May 19 and June 6, 2006 (set-up day). June was also relatively dry with the only rainfall occurring between June 6 and June 9 (16 mm) and between June 24 and June 28 (25.2 mm). The monsoon season started in July, after the end of the experiment.

The instruments were elevated on two slopes that overlook the relatively flat grassland (Fig 2a). In each valley slope receivers and transmitters were spatially alternated to form adjacent pairs of LAS transects. The distance between the outermost LASs on the same side of the transect (LAS 32 and 31) was 53.9 m at the north-west end, and 26.2 m at the south-east end. For experiment H2 the order of LAS transects from experiment H1 was inverted. The order from north to south of the transects in experi-

ment H1 was '31, '17, '05, '15, '32 and changed to '32, '15, '05, '17, '31 for experiment H2 (Fig. 2a) . As a result transect '05 was not changed between H1 and H2, but '31 was exchanged for '32, and '15 was exchanged for '17. Within a transect, the receiver was not switched with the transmitter, i.e. an instrument that was located at the north-west side during experiment H1 remained there for experiment H2. This resulted in identical transect geometries but different instruments, enabling us to control for the effects of slightly different footprint and transect geometry (especially beam height) and focus on comparing instruments.

Two hundred waypoints were taken with a Global Positioning System (GPS) Wide Area Augmentation System (WAAS) to establish the transect profile and the beam height. The absolute accuracy of GPS-WAAS is $\approx$ 1 m or 2% of the beam height. Special care was taken to accurately determine the relative height of the transmitters and receivers. Differential GPS (DGPS) measurements were taken and confirmed by laser level measurements resulting in accuracies of $\approx$ 0.1 m or 0.2% in relative height of the five beams. Errors in the transect length are 2 m or better and can be neglected (Hartogensis et al. 2003). An eddy-covariance (EC) energy balance tower was located 1.3 km south of the transect over homogeneous grassland (grass height 0.3-0.5 m) similar to the vegetation in the footprint of the LAS, and it was instrumented with a Licor Li7500 open path CO_2/H_2O infrared gas analyzer (IRGA), a Campbell Scientific 3D sonic anemometer (CSAT3) at 2.93 m above ground level (a.g.l.), a Kipp and Zonen NR-Lite net radiometer, and a tipping bucket rain gauge. The 20 Hz EC data were stored and corrected for coordinate rotation, frequency response, and Massman correction in postprocessing using 30-min averages. From the EC measurements, roughness length and zero displacement height were determined as $z_o = 0.014$ m and $d = 0.01$ m (Martano 1999).

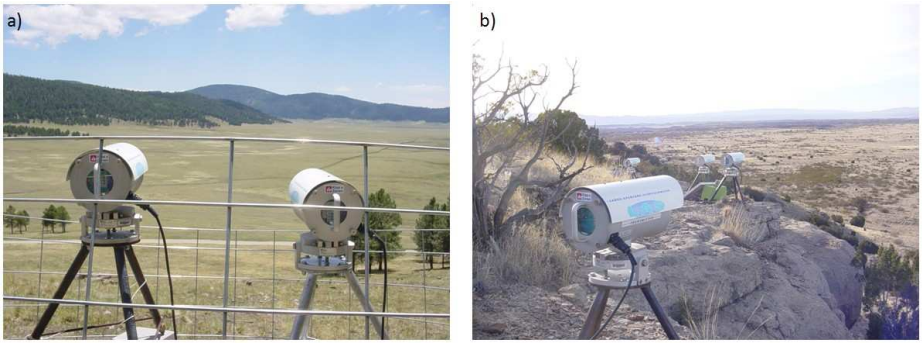

Fig. 1 Photographs of experiments at sites. a) Valles Caldera National Preserve: north-west end of the transects of experiment H1 looking south-east. The instruments at the other end of the transect are invisible in a clearing on the opposite site of the valley. b) Sevilleta National Wildlife Refuge: south-east (transmitter) end of the transects of experiment S4 looking south-west. Receivers are out of the photograph to the right.

2.3 Slant Beams at the Sevilleta National Wildlife Refuge (SNWR)

Four Kipp and Zonen LASs were set up over arid shrubland in the Sevilleta National Wildlife Refuge (SNWR), 80 km south of Albuquerque, New Mexico from November 18, 2005 to March 31, 2006 (Table 1, Fig. 3). Mean daily maximum and minimum air temperatures during the study were 14.8 ^oC and -3.4 ^oC, respectively. The transmitters were located on a ridge, near $34^o16.618'$ N, $-106^o39.282'$ W (WGS84), and the receivers were located 80 m lower in the plains at a bearing of $\approx 295^o$ from the receivers, resulting in slanted transects. The transect length L was varied between 1266 m and 2846 m.

The transect profiles were measured with a GPS-WAAS and the height differences between the four receivers (all experiments) and four transmitters (experiment S4 only, the large transmitter spacing for experiments S1-S3 exceeded the range of the laser-level) were measured with a laser-level. Thus expected relative accuracies in z_{eff} were

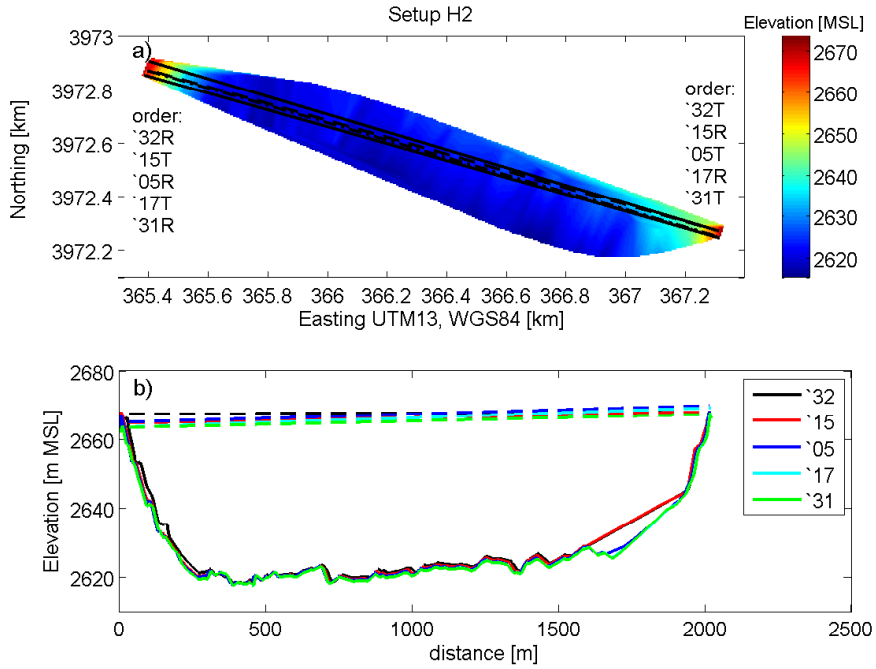

Fig. 2 a) Bird's eye view of the digital elevation model (DEM) of the VCNP experiment H2 with LAS transects. The legend gives the last two digits of the LAS serial number (Table 1). The EC tower coordinates are 366.7 E and 3971.1 N (UTM13, WGS84). Receivers and transmitters were alternated at each site. (b) Profile of transects.

0.1 m (corresponding to 0.5% of z_{eff}) or better for experiment S4 and 1 m (corresponding to 6% of z_{eff}) for the other experiments.

The EC technique was used to obtain the sensible and latent heat fluxes near the center of the transect. A CSAT3 and Krypton Hygrometer (KH2O) were mounted at a height of 2.85 m AGL and connected to a CR10X datalogger sampling at 8 Hz. Measurements on the EC tower also included net radiation (Q7 at 2.7 m, Radiation Energy Balance Systems Inc.), soil heat flux (Hukseflux self-calibrating heat flux plate at -0.06 m), and soil temperature (thermocouple at -0.03 m). From the EC measure-

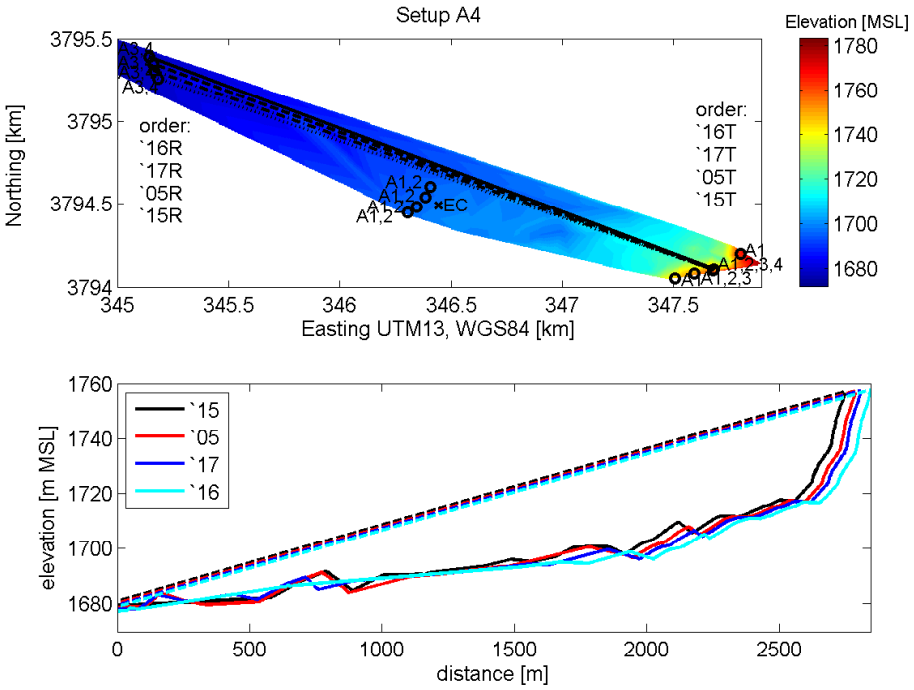

Fig. 3 a) Bird's eye view of a digital elevation model (DEM) of the Sevilleta NWR set-up area with LAS transects of experiment S4 (lines). The legend gives the last two digits of the LAS serial number (Table 1). The locations of the transect endpoints of experiments S1-S3 are shown as circles, where adjacent numbers denote the experiment number. All transmitters were on the south-east (high) end of the transect, and all receivers were on the north-west end of the transect. (b) Profile of S4 transects.

ments, roughness length and zero displacement height were determined as $z_o = 0.026$ m and $d = 0.01$ m.

3 Methods

The LAS measures light intensity fluctuations that are caused by variations of the refractive index of air n. The LAS electronics compute internally the structure parameter of the refractive index, C_n^2, which is a function of both temperature and humidity fluc-

tuations. The derivation of the sensible heat flux from C_n^2 is described in this section. Required geometrical (transect length and height) and other parameters are listed in Table 2.

3.1 Derivation of the sensible heat flux

Firstly, to obtain C_n^2, Eq. 1 has to be applied to correct the output from the scintillometer ($C_{n,\mathrm{pot}}^2$) for the difference between geometric aperture diameter D and effective aperture diameter D_{eff} and for the difference in the potentiometer setting L_{pot} from the actual transect length L as $C_n^2/C_{n,LAS}^2 = (D/D_{\mathrm{eff}})^{7/3}(L/L_{\mathrm{pot}})^{-3}$. If L and D_{eff} were known a priori and the receiver's potentiometer was set correctly this step could be avoided. The manufacturer advises use of this equation only to correct for small differences between L and L_{pot} ($\approx$ 20 m, depending on L). Then, C_T^2 can be derived from C_n^2 as follows (Wesely 1976):

$$C_T^2 = \left(\frac{-0.78\times10^{-6}p}{T^2}\right)^{-2} C_n^2 \left(1+\frac{0.03}{BR}\right)^{-2} \approx \left(\frac{-0.78\times10^{-6}p}{T^2}\right)^{-2} C_n^2 \quad (2)$$

where p is air pressure [Pa] and T [K] is air temperature. The last equality holds for dry conditions or a large Bowen Ratio (BR), when humidity fluctuations do not contribute significantly to refractions of the LAS beam (for $BR = 2$ and $BR = 0.6$ and standard temperature and pressure the correction factor $(1 + 0.03/BR)^2$ is 1.03 and 1.10, respectively). At the SNWR site, no rainfall occurred during the experiment, and in the absence of significant transpiration BR was large ($BR > 3$) and the influence of humidity fluctuations on the structure parameter of the refractive index was negligible. Since the daytime BR at the VCNP EC tower were typically between 0.7 and 2 we used a constant $BR = 1$ in Eq. 2. Due to horizontal homogeneity over the footprint

areas of the five LAS transects the BR correction factors (and the associated errors) are expected to be the same for all transects. For comparisons between LAS and EC, errors in BR during experiment H1-H2 could contribute at most an error in C_n^2 of 3.5% (Section 4.3).

Once C_T is known, the sensible heat flux can be obtained iteratively from the following system of equations (Wyngaard et al. 1971)

$$\frac{C_T^2 (z_{\text{eff}} - d)^{2/3}}{T_*^2} = f_T(\zeta), \tag{3}$$

$$T_* = \frac{-H}{\rho_{\text{air}} c_p u_*}, \tag{4}$$

$$L_{\text{MO}} = \frac{u_*^2 T}{g \kappa T_*}, \tag{5}$$

where $f_T(\zeta) = c_1(1 - c_2\zeta)^{-2/3}$ and $f_T(\zeta) = c_1(1 + c_3\zeta^{2/3})$ are the universal stability functions for unstable and stable conditions, respectively (Wyngaard et al. 1971; Andreas 1988; de Bruin et al. 1993), $\kappa = 0.4$ is the von Karman constant, $\zeta = (z_{\text{eff}} - d)/L_{\text{MO}}$, and $c_1 = 4.9$, $c_2 = 6.1$, $c_3 = 2.2$. The friction velocity u_* is derived from estimates of z_o, d, the integrated flux profile relationships (Panofsky and Dutton 1984), and measurements of the mean horizontal wind speed.

Since the direction of the heat flux cannot be inferred from LAS measurements, initially one stable and one unstable solution are derived for each time interval. Our sites were typically not exposed to advection of warm air, which would produce negative daytime sensible heat fluxes. Thus the transition between unstable and stable conditions occurs near sunrise and sunset, when the net radiation changes sign. The near-neutral conditions associated with a sign change in H cause local minima in C_n^2. Thus the detection of the transition can be automated, but in practice visual inspection

Table 2 Auxiliary measurements for the derivation of the sensible heat flux from C_n^2 and for cross-comparison to EC measurements.

Variable	Sevilleta NWR	Valles Caldera NP
wind speed and direction	CSAT3 near transect center	CSAT3 1.3 km south of transect
air temperature	CSI108 at Rec, z = 1.5 m AGL	HMP45C 1.3 km south of transect
air pressure	polytropic vertical interpolation from hourly AWOS at ABQ	Li7500
roughness length	0.026 m	0.014 m
Bowen ratio	3	1
EC sensible heat flux	CSAT3 and KH2O (10-min mean)	CSAT3 and Li7500 (30-min mean)

is still required since occasionally the nighttime minimum in C_n^2 is smaller than the minimum at the transition from stable to unstable or vice versa.

3.2 The effective beam height

A relative error in z_{eff} will result in at least half that relative error in H, so accurate determination of z_{eff} is therefore critical but difficult over non-flat terrain. The effective height depends on stability (Eq. 12 in Hartogensis et al. 2003), and thus needs to be solved together with the system of Equations 3–5, resulting in a different z_{eff} for each averaging interval. Equations 3–5 were first solved using the free convective solution for z_{eff} (Eq. 13 in Hartogensis et al. 2003)

$$z_{\text{eff}} = \left[\int_0^1 Z(x')^{-4/3} G(x') dx' \right]^{-3/4}, \quad (6)$$

$$G(x') = \frac{W(x')}{\int_0^1 W(x') dx'}, \quad (7)$$

$$W(x') = 16\pi^2 K^2 L \int_0^\infty k\phi_n(k) \sin^2\left[\frac{k^2 L x'(1-x')}{2K}\right] \left[\frac{2J_1(x_1)2J_1(x_2)}{x_1 x_2}\right]^2 dk, \quad (8)$$

where K is the optical wavenumber, k is the spatial wavenumber, $\phi_n(k)$ is the three-dimensional spectrum of refractive index fluctuations, J_1 is the Bessel function of the first kind with $x_1 = kDx'/2$ and $x_2 = kD(1-x')/2$, $x' = x/L$ is non-dimensional distance, Z is beam height a.g.l., and L is the transect length. The LAS locations and the transect profile were obtained from GPS-WAAS readings (see Figs. 2, 3 for the digital elevation model obtained from the GPS-WAAS waypoints). Then, using the Obukhov length L_{MO} derived from Eq. 5, the effective beam height was recalculated using the stability dependent solution for z_{eff} (Eq. 12 in Hartogensis et al. 2003). In the Appendix we show that the solution for z_{eff} in stable conditions is identical to the solution for neutral conditions, i.e. $z_{\mathrm{eff,stable}} = \left(\int_0^1 Z(x')^{-2/3} G(x') dx'\right)^{-3/2}$. At the VCNP site the difference in the effective height between the free convective and neutral solutions was less than 0.15 m or 0.35%.

3.3 Data filters

As suggested in the Kipp and Zonen LAS manual, data were not used when the signal strength ("demod") fell below 50 mV. Due to insufficient solar panel size and associated power outages, this happened frequently at night. For the intercomparison, only unstable daytime data are shown. Finally, for the comparison between LAS and EC measurements, wind direction filters were applied to exclude CSAT data from a 60^o sector in the rear of the sensor and tower.

4 Results

A measurement intercomparison could be performed for the parameter that is measured directly from the LAS (σ_{lnI}) or derived without external measurements (C_n^2). However, identical C_n^2 measurements could only be expected if z_{eff} was identical, since C_T^2 scales approximately with $z_{\text{eff}}^{-4/3}$. Rather than comparing rescaled measurements of C_n^2, we chose to present the comparisons in terms of sensible heat fluxes (Eq. 3) because meteorologists and hydrologists are more familiar with this variable. Since identical parameters (z_o, T, U, BR) were used to compute H from C_n^2, the regression results are expected to be comparable to regressions using a rescaled C_n^2.

From linear regressions between 10-min averages of H from two instruments (LAS,ref and LAS) we obtain the regression equation $H_{\text{LAS}} = aH_{\text{LAS,ref}}$, the mean absolute deviation as mean$\left|H_{\text{LAS,ref}} - H_{\text{LAS}}\right|$, and the correlation coefficient $\rho(H_{\text{LAS,ref}}, H_{\text{LAS}})$. To obtain an estimate for the difference between any two LASs, we computed the median of all normalized differences for LASs i at all times t, $\Delta_i(t)$

$$\Delta_i(t) = \left[H_{\text{LAS,i}}(t) - AVG(H_{\text{LAS,i}}(t))\right] / AVG(H_{\text{LAS,i}}(t)), \tag{9}$$

where AVG($H_{\text{LAS,i}}(t)$) is the mean of all LAS sensible heat fluxes in the 10-min interval centered at time t. Since the normalized differences are nearly constant in time for a given experiment, the median of $\Delta_i(t)$ is close to the median of differences in linear regression slopes (Tables 3 and 4 later). We chose the median instead of the average, since $\Delta_i(t)$ goes to infinity for AVG(H_{LAS}) going to zero, as is the case around sunrise and sunset.

A representative example of the resulting time series of sensible heat fluxes from experiment H1 is shown in Fig. 4. Qualitatively the LAS and EC measurements agree

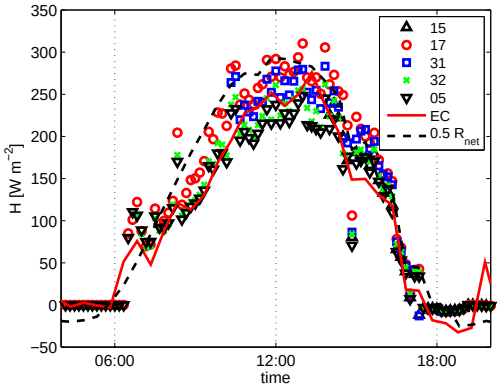

Fig. 4 Example time series of the net radiation (R_{net} rescaled by 1/2) and sensible heat flux H from LAS and EC for experiment H1 on June 19, 2006.

well in stable and unstable conditions. Short-term fluctuations in H due to net radiation changes (e.g. at about 1445h local time in Fig. 4) can be captured with the LAS due to the short averaging time scale of 10 min. In this section we will first present intercomparisons of LAS measurements over nearly identical transects and then present intercomparisons of measurements in the same ecosystem, but somewhat different z_{eff} and location. This choice is motivated by the fact that (a) natural surfaces always display some degree of heterogeneity, and (b) errors in the GPS measurements of z_{eff} may induce errors in the computation of H. Thus, if LASs are not set up directly adjacent to each other, disagreements may be partially explained by vegetation or soil heterogeneity in the flux footprint areas or errors in z_{eff}.

For the LAS intercomparison of S1-4 and H1-2, the instruments with serial number $^{0500}17$ and $^{0300}05$ were chosen as the reference measurement, respectively. While this choice was random for S1-S4, $^{0300}05$ was chosen for H1-2, since it was the only LAS that was not moved during the field campaign.

4.1 Intercomparison of LASs over identical transects

The measurements from experiments H1 and H2 allow for the best examination of the uncertainties due to transect geometry versus real instrument differences. The order of the transects was 'inverted' between H1 and H2, while the positions and all external measurement hardware, such as dataloggers, were the same.

Figure 5 shows the scatter plots for the unstable sensible heat fluxes obtained from five LASs during H1. The figure shows high correlation coefficients of greater than 0.995, which are much larger than those from intercomparisons of EC measurements (average R^2 for rotated $w'T'$ of 0.94, Loescher et al. 2005). However, the linear regression reveals significant differences between LASs. While the differences are only 6% or less between LAS '15, '32 and '05, larger differences of up to 21% were obtained for LASs '31 and '17. The regression slopes and correlation coefficients for H2 (table 3) are similar to those from H1 and the ranking of different sensors is identical, even though their position had changed.

The set-up locations for S1-S4 were less ideal for an instrument intercomparison than H1 and H2. The slanted transects (Fig. 3b) and the spacings of 30 m in between any two receivers caused (small) differences in footprint location and z_{eff}. Unlike S1 and S2, in S3 and S4 at least the four transmitters were set up less than 5 m away from each other (Fig. 1b and 3a) allowing comparisons of the sensible heat flux over nearly identical transects. Between S3 and S4 the order of the transects was inverted (similar to that done for H1 and H2), but road construction work at the site did not permit using the exact same locations for the receivers. For S3 and S4, the regression slopes ranged from 1.05 to 1.25 (Fig. 6), while the relative ranking of different sensors was the same for both experiments. LAS ^{0500}15 showed higher values than LAS ^{0500}16,

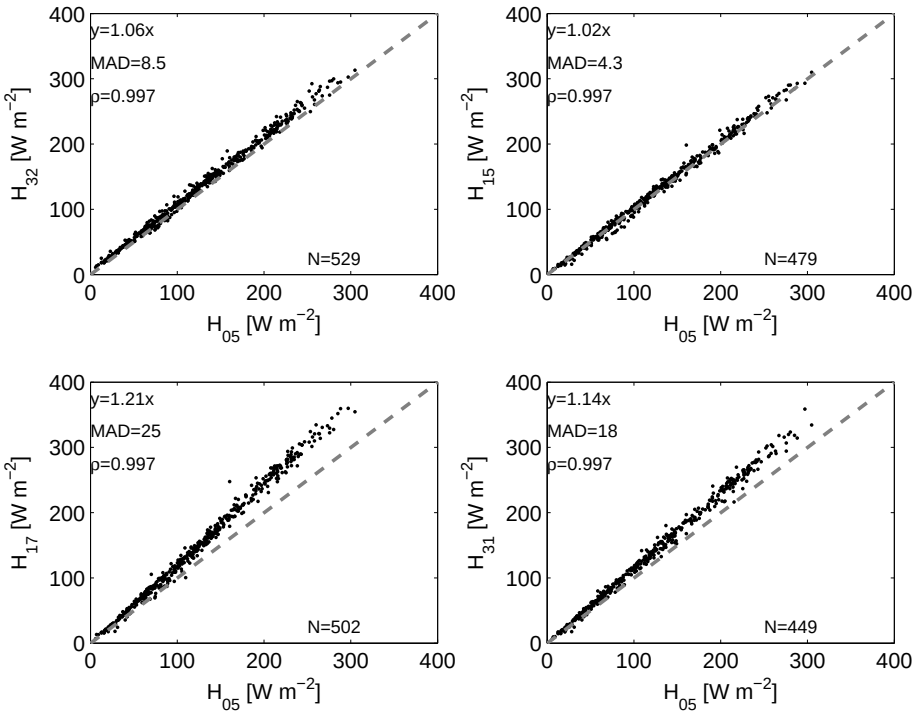

Fig. 5 Scatter plots of sensible heat flux measurements from serial number $^{0300}05$ (x-axis) vs the other LASs (only the last two digits of the serial number are shown in the axis labels) for experiment H1. The text indicates the linear fit, mean absolute deviation (MAD in W m^{-2}), correlation coefficient ρ, and number of samples N. The grey dashed line is the 1:1 line.

which in turn showed larger values than LAS $^{0500}17$. As mentioned in Section 2.3., a difference of up to 3% could be explained by uncertainties in the estimation of z_{eff} for each transect, but the observed differences are significantly larger. No explanation for the variation of the regression slope of LAS $^{0500}15$ between S3 and S4 can be offered.

4.2 Intercomparison of LASs over non-identical transects

Experiments S1-S2 were designed to examine the influence of transect location and geometry on the accuracy of sensible heat flux measurements with scintillometry. In S1

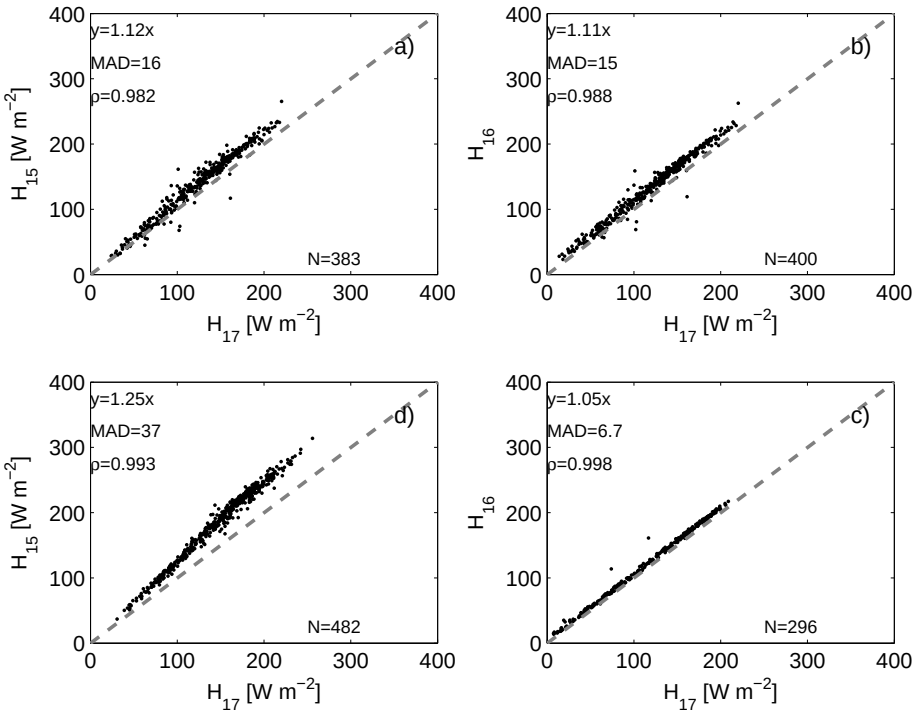

Fig. 6 Same as Fig. 5 for experiments S3 (a, b) and S4 (c, d).

and S2, z_{eff} and the lateral spacing varied more than in S3 and S4. Thus the differences found in the intercomparison of S1 and S2 are the combined effect of instrument error in C_n^2, measurement error in the transect geometry parameters, and natural variation of H over different footprints in a seemingly homogeneous area. The receiver locations for S1 and S2 were identical, but in S1 the transmitters were spread out over a distance of 0.4 km, while in S2 the two outer transmitters were moved adjacent to the two inner transmitters to form two pairs of two adjacent transects. Despite the larger transect separation, the correlation coefficients remained comparable to S3 and S4 at an average of $\rho = 0.987$ (figures omitted for brevity). Also no significant difference between the regression slopes of the transects whose transmitters were moved between S1 and S2 were found, indicating the homogeneity of surface and robustness of the measurement

at different locations. The ranking of the instruments' H measurements was consistent with the ranking in S3 and S4.

4.3 Intercomparison of LAS and EC

A perfect match between LAS and EC measurements is not expected, since the LASs were at a different location (for H1 and H2) and greater height (20-45 m vs. 3 m) and thus the LAS footprints were displaced and much larger than the EC footprint. Absolute errors in z_{eff} for the LASs may also contribute to EC-LAS differences in H. Moreover, only one EC station was deployed for each experiment, resulting in significant uncertainties in H_{EC} (Loescher et al. 2005). However, LAS-EC comparisons provide a point of reference especially relevant in light of the discussion of energy balance closure problems with EC measurements.

Data from S3 are shown as an example of the LAS-EC intercomparison (Fig. 7), since these EC measurements were taken close to the centre of the transects (Fig. 3a), the measurement height was closer to the LAS beam, and the EC and LAS averaging times were consistent at 10 min. As expected the correlation coefficients are lower than for LAS-LAS intercomparisons at around $\rho = 0.94$. LAS sensible heat fluxes were 2-17% larger than those from EC, which would result in an improved energy balance closure. Considering experiments S1-S4, the regression slopes $H_{\mathrm{LAS}} = aH_{\mathrm{EC}}$ ranged from 0.95 to 1.39 with an average of 1.16 (not shown). For the horizontal path experiments the slopes ranged from 0.86 to 1.12 with an average of 0.99.

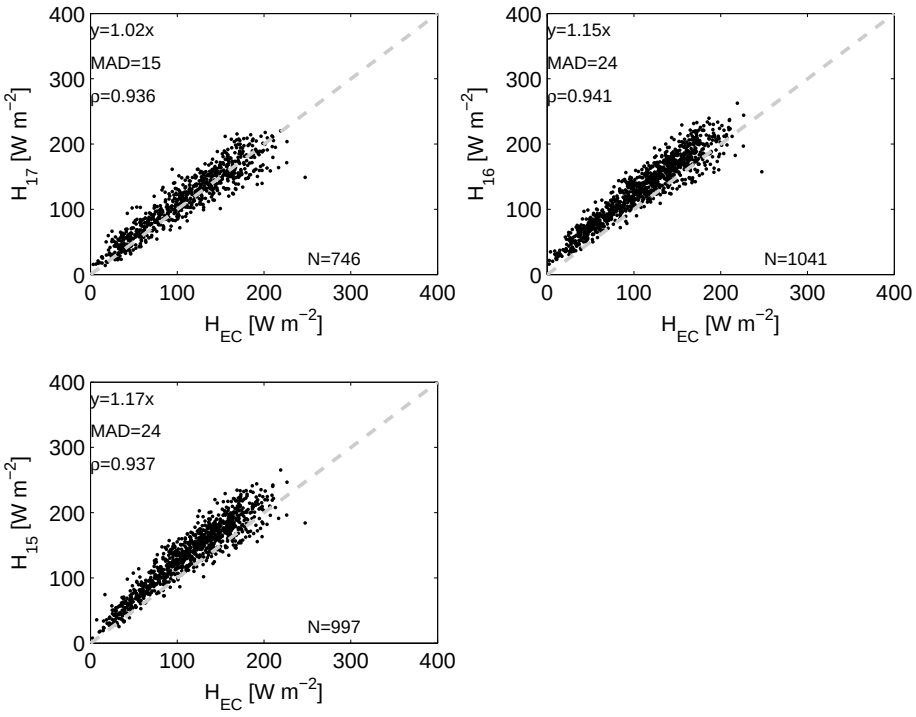

Fig. 7 Scatter plots of sensible heat flux measurements from eddy-correlation (H_{EC}) versus different LASs (only the last two digits of the serial number are shown in the axis label) for experiment S3. The figure also shows the linear fit, mean absolute deviation (MAD in W m^{-2}), correlation coefficient ρ, and number of samples N.

5 Discussion and conclusions

The advantage of the LAS compared to the EC system lies in the scintillometer as a remote sensor that uses spatial averaging of light intensity fluctuations to derive the structure parameter of the refractive index. A disadvantage is that LAS sensible heat flux measurements rely on similarity theory requiring the measurement of additional parameters to derive the sensible heat flux H from C_n^2. In this study we did not examine the validity of MOST, but used instrument intercomparisons to establish consistency

of the LAS technology. The regression slopes and confidence intervals of all instrument intercomparisons are summarized in Tables 3 and 4.

Random errors in 10-min averages of H_{LAS} measurements were small since the correlation coefficients between adjacent measurements were greater than 0.995. However, linear regression of H_{LAS} showed significant inter-instrument differences in the regression slopes (i.e. the gain) that resulted in a difference in C_n^2 and H. Experiments H1 and H2 in the Valles Caldera National Preserve grassy highlands (Table 3) allowed us to examine the reasons for the differences since the set-up locations were identical, with only the order of instruments changed. The regression slopes changed only slightly between H1 and H2, indicating that errors due to location, effective height z_{eff}, or external devices (e.g. dataloggers) were not responsible for the majority of the observed differences. If errors in z_{eff} were responsible, then, for example, the regression slope for LAS $^{0500}15$ should have changed from 1.02 to 1.21, which was the slope for LAS $^{0500}17$ in H1 (LAS transect $^{0500}15$ and LAS $^{0500}17$ exchanged places between H1 and H2).

For the slant path experiment in the arid Sevilleta National Wildlife Refuge (Table 4), the differences in the regression slopes between LASs were up to 25% for experiments S3 and S4, and up to 40% (slope of LAS $^{0500}15$ divided by slope of LAS $^{0300}05$, $1.19/0.85 = 1.4$) for S1 and S2 . The ranking of LASs by regression slope was constant, indicating that the differences must be partially caused by true instrument differences, while some of the differences may be caused by inaccurate z_{eff} measurements and differences in footprint.

With the exception of LAS $^{0500}15$ (to be discussed later), the results from the slant path (S1-4) and horizontal path (H1-2) experiments agree, both in regression and correlation coefficients. Thus accurate LAS measurements can be conducted over

Table 3 Linear regression slopes and 95% confidence intervals of sensible heat fluxes between LAS-LAS and LAS-EC for the experiments H1 and H2 in unstable conditions.

	LAS '32	LAS '15	LAS '05	LAS '17	LAS '31	median(Δ)
LAS '05 - H1	$1.06 \pm .01$	$1.02 \pm .01$	1	$1.21 \pm .01$	$1.14 \pm .01$	.063
LAS '05 - H2	$1.11 \pm .01$	$1.04 \pm .01$	1	$1.16 \pm .01$	$1.14 \pm .01$	.053
EC – H1	$0.91 \pm .06$	$0.87 \pm .06$	$0.86 \pm .05$	$1.04 \pm .06$	$0.96 \pm .06$	
EC – H2	$1.05 \pm .12$	$1.01 \pm .09$	$0.96 \pm .10$	$1.12 \pm .11$	$1.10 \pm .10$	

Table 4 Same as Table 3 for experiments S1-S4

	LAS '17	LAS '05	LAS '15	LAS '16	median(Δ)
LAS '17 - S1	1	$0.85 \pm .02$	$1.16 \pm .05$	$1.05 \pm .02$	.092
LAS '17 - S2	1	$0.85 \pm .02$	$1.19 \pm .02$	$1.07 \pm .01$	.107
LAS '17 - S3	1	X	$1.12 \pm .02$	$1.11 \pm .02$	.045
LAS '17 - S4	1	X	$1.25 \pm .01$	$1.05 \pm .01$	.095
EC – S1	$1.19 \pm .07$	$1.01 \pm .07$	$1.39 \pm .08$	$1.25 \pm .07$	
EC – S2	$1.13 \pm .04$	$0.95 \pm .04$	$1.33 \pm .07$	$1.27 \pm .04$	
EC – S3	$1.02 \pm .02$	X	$1.17 \pm .02$	$1.15 \pm .02$	
EC – S4	$1.01 \pm .04$	X	$1.26 \pm .04$	$1.06 \pm .03$	

slant paths, so long as beam heights are measured accurately over the transect and stability-dependent effective heights are computed.

The median of inter-instrument differences (Eq. 9) is given in the last column of Tables 3 and 4. This measure of typical inter-instrument differences is about 6% for the ideal experiment H1 and H2 and around 10% for S1-S4. To explain these unexpectedly large differences, we quantified two other sources of error related to the optics and electronics: (1) the error in setting the path length potentiometer and in calibration

of electronics; and (2) differences in the effective diameter of the LAS transmitter and receiver.

Moene et al. (2005) examined different sources of errors in the LAS electronics. Tolerances of electronic components can account for only up to 3% error in C_n^2. Manually setting the path length using the potentiometer dial ($\mathrm{Pot_{LAS}}$) represents a change in the electronic gain and has the advantage that C_n^2 can be output directly from the LAS' analog circuit (an alternative approach would be to store raw time series of the demodulated signal and determine C_n^2 from the raw data in postprocessing). The manufacturer calibrates this gain as function of path length from the LAS optics equations and the design of the electronics (Moene et al. 2005). If not corrected in data processing using Eq. 1, incorrectly setting $\mathrm{Pot_{LAS}}$ will cause slope differences such as those observed in our study . The scale of the dial of the path length potentiometer $\mathrm{Pot_{LAS}}$ (range 0-1000) is small and therefore also sensitive to errors in reading the setting, which enters in Eq. 1. The percentage error in C_n^2 that is introduced due to an error of 1 in $\mathrm{Pot_{LAS}}$ is $\approx 1\%$ for typical path lengths of 500-2500 m (Fig. 3.3 of Moene et al. 2005). Large $\mathrm{Pot_{LAS}}$ mis-settings in experiments S3 and S4 (up to 25 less than their optimal value) may have contributed to the difference in the regression slopes from 1, since little is known about the accuracy of corrections for large missettings. However, the $\mathrm{Pot_{LAS}}$ settings for the S1, S2, H1, and H2 were within one of the optimal setting and thus are not expected to be significant sources of error.

The geometric diameter of the lenses used in the LAS receiver and transmitter is 0.152 m. However, the quality of the lenses, the radiation pattern of the light emitting diode (LED), and viewing pattern of the photodiode all influence the effective diameter D_{eff} (i.e. beam diameter) of the LAS transmitter and receiver. According to the manufacturer of the LED, the radiation pattern is stable in the range of -26 to

+26 degrees used in the LAS so that D_{eff} should not be affected. It has been observed by Kipp and Zonen (also in the instrument $^{0500}15$ used in this study) that there is significant variation in the focal length of the Fresnel lenses. It is possible that this and other non-uniform properties of the lenses affect D_{eff}.

D_{eff} can be determined experimentally by placing different apertures in front of the transmitter or receiver and plotting the relation between the square root of signal strength and aperture diameter. Conducting this test for a pre-commercial set of LASs using apertures of 0.075 m, 0.10 m, 0.125 m, 0.140 m and 0.152 m, Kipp and Zonen (unpublished manuscript) found that D_{eff} is approximately 0.148 m for the receiver and 0.145 m for the transmitter, suggesting that the viewing pattern of the photodiode is slightly better than the radiation pattern of the LED. In Eq. 1 the average $D_{\text{eff}} = 0.1465$ m is used. A decrease of 2 mm in D_{eff} results in a decrease of H (and C_n) by $\approx 2\%$ (Eq. 1) indicating a large potential for errors.

It is unknown whether there are significant inter-instrument differences in D_{eff}. Furthermore, it is not known what happens to D_{eff} when the LED or photodiode is out of focus. We experienced technical problems with transmitter $^{0500}15$ during S1-S4. The distance between photodiode and lens inside transmitter $^{0500}15$ had been set incorrectly by the factory resulting in the photodiode being out of focus. Thus this transmitter had to be operated at much higher power settings (typically 2-3 times the power setting of other LASs) and was sent for repair after S4. LAS $^{0500}15$ worked normally during H1 and H2. Interestingly, H from LAS $^{0500}15$ was on average 18% larger than LAS $^{0500}17$ while the photodiode was out-of-focus during experiments S1-S4. After the repair H from LAS $^{0500}15$ was on average 18% smaller than LAS $^{0500}17$. Kipp and Zonen is investigating these issues, but considering the large sensitivity of

the C_n^2 measurements to the effective diameter (Eq. 1) we consider uncertainty in D_{eff} as a prime suspect for the large differences that we observed.

In summary, significant inter-instrument differences in sensible heat fluxes were found. In carefully controlled experiments, this difference was as large as 21%, but typically on the order of ±6% (as measured by the median of inter-instrument differences). Errors of ±10% are typical in more realistic measurement scenarios over homogeneous natural vegetation and different transect heights and locations. To obtain errors relative to true sensible heat fluxes, errors in the auxiliary variables used to compute H (Table 2 and transect geometry) have to be taken into account, which Hartogensis et al. (2003) estimated to be on the order of 10%. Error propagation using our 6% consistency error estimate and the 10% error estimate of Hartogensis et al. (2003) results in a total error of 12%.

High correlation coefficients between different instruments even over displaced transects suggest that the scintillometer technique is robust, but care has to be taken by the manufacturer to ensure accurate performance of the optics and electronics of the LAS. The small aperture or laser scintillometer is in advantage, since no aperture is used and thus the effective diameter is not required for data processing. For multi-instrument studies it is recommended to conduct intercomparison measurements between the different LASs for detection and correction of instrument gains in sensible heat fluxes measurements. Future work will include the comparison of LAS from different manufacturers.

Acknowledgements The following sponsors have contributed to this study: NSF EPSCoR grant EPS-0447691; U.S. Department of Agriculture, CSREES grant No.: 2003-35102-13654; and the NSF Science and Technology Center program Sustainability of Semi-Arid Hydrology and Riparian Areas (SAHRA; EAR-9876800). We are indebted to the Sevilleta National

Wildlife Refuge staff and affiliated scientists, in particular Renee Robichaud, Don Natvig, Renee Brown, and Mike Friggens for assistance with preparation and execution of the experiment. Without Bob Parmenter, Johnny, Albert, and Juglio of the Valles Caldera National Preserve our experiment would not have been possible. Assistance in the field by Kathy Fleming, Kimberly Bandy, and Jack Cheney is acknowledged.

6 Appendix: The effective beam height for stable conditions

We substitute the equation for f_T under stable conditions $f_T\left(z/L_{\mathrm{MO}}\right) = c_1\left[1 + c_3\left(z/L_{\mathrm{MO}}\right)^{2/3}\right]$ into Eq. 12 of Hartogensis et al. (2003):

$$z_{\mathrm{eff}}^{-2/3} f_T\left(\frac{z_{\mathrm{eff}}}{L_{\mathrm{MO}}}\right) = \int_0^1 Z^{-2/3} f_T\left(\frac{Z}{L_{\mathrm{MO}}}\right) G du, \tag{10}$$

Then rewrite the left-hand side (LHS) and right-hand side (RHS) of this equation:

$$LHS = c_1 z_{\mathrm{eff}}^{-2/3}\left[1 + c_3\left(\frac{z_{\mathrm{eff}}}{L_{\mathrm{MO}}}\right)^{2/3}\right] = c_1\left[z_{\mathrm{eff}}^{-2/3} + c_3 L_{\mathrm{MO}}^{-2/3}\right], \tag{11}$$

$$RHS = c_1\int_0^1 Z^{-2/3}\left[1 + c_3\left(\frac{Z}{L_{\mathrm{MO}}}\right)^{2/3}\right] G du = c_1\int_0^1 Z^{-2/3} G du + c_1 c_3 L_{\mathrm{MO}}^{-2/3} \tag{12}$$

Thus, the effective height for stable conditions is $z_{\mathrm{eff}} = \left[\int_0^1 Z^{-2/3} G du\right]^{-3/2}$.

References

1. Andreas, E., 1988: Estimating C_n^2 over snow and sea ice from meteorological data. *J. Opt. Soc. Amer.*, **5**, 481–495.
2. — 1990: Selected papers on turbulence in a refractive medium. *SPIE - The International Society for Optical Engineering, Bellingham.*, **25**, 1–693.
3. Asanuma, J. and K. Iemoto, 2007: Measurements of regional sensible heat flux over Mongolian grassland using large aperture scintillometer. *J. Hydrol.*, **333**, 58–67.

4. Beyrich, F., H. de Bruin, W. Meijninger, J. Schipper, and H. Lohse, 2002: Results from one-year continuous operation of a large aperture scintillometer over heterogeneous land surface. *Bound.-Layer Meteorol.*, **105**, 85–97.

5. Clifford, S., G. Ochs, and R. Lawrence, 1974: Saturation of optical scintillation by strong turbulence. *J. Opt. Soc. Amer.*, **64**, 148–154.

6. de Bruin, H., 2002: Introduction: Renaissance of scintillometry. *Bound.-Layer Meteorol.*, **105(1)**, 1–4.

7. de Bruin, H., W. Kohsiek, and B. van den Hurk, 1993: A verification of some methods to determine the fluxes of momentum, sensible heat, and water vapor using standard deviation and structure parameter of scalar meteorological quantities. *Bound.-Layer Meteorol.*, **63**, 231–257.

8. de Bruin, H., B. van den Hurk, and W. Kohsiek, 1995: The scintillation method tested over a dry vineyard area. *Bound.-Layer Meteorol.*, **76**, 25–40.

9. der Molen, M. V., J. Gash, and J. Elbers, 2004: Sonic anemometer (co)sine response and flux measurement. II. the effect of introducing an angle of attack dependent calibration. *Agric. For. Meteorol.*, **122**, 95–109.

10. Foken, T., F. Wimmer, M. Mauder, C. Thomas, and C. Liebethal, 2006: Some aspects of the energy balance closure problem. *Atmos. Chem. Phys. Discuss.*, **6**, 3381–3402.

11. Gash, J. and A. Dolman, 2003: Sonic anemometer (co)sine response and flux measurement. I. the potential for (co)sine error to affect sonic anemometer-based flux measurements. *Agric. For. Meteorol.*, **119**, 195–207.

12. Hafeez, M., M. Andreini, J. Liebe, J. Friesen, A. Marx, and N. Giesen, 2006: Hydrological parameterization through remote sensing in Volta basin, West Africa. *Intl. J. River Basin Management*, **4**, 1–8.

13. Hartogensis, O., C. Watts, J.-C. Rodriguez, and H. de Bruin, 2003: Derivation of an effective height for scintillometers: La Poza experiment in northwest Mexico. *J. Hydrometeorol.*, **4**, 915–928.

14. Hemakumara, H., L. Chandrapala, and A. Moene, 2003: Evapotranspiration fluxes over mixed vegetation areas measured from a large aperture scintillometer. *Agric. Water Management*, **58**, 109–122.

15. Hendrickx, J., J. Kleissl, J. Gomez-Velez, S.-H. Hong, J. Fabrega-Duque, D. Vega, H. Moreno-Ramirez, and F. Ogden, 2007: Scintillometer networks for calibration and validation of energy balance and soil moisture remote sensing algorithms. *Proc. International Society for Optical Engineering*, **6565**, 65650W.

16. Hill, R., 1997: Algorithms for obtaining atmospheric surface-layer fluxes from scintillation measurements. *J. Atmos. Oceanic Technol.*, **14**, 456:467.

17. Hill, R., G. Ochs, and J. Wilson, 1992a: Measuring surface-layer fluxes of heat and momentum using optical scintillation. *Bound.-Layer Meteorol.*, **58**, 391–408.

18. — 1992b: Surface layer fluxes measured using the CT2-profile method. *J. Atmos. Oceanic Tech.*, **9**, 526–537.

19. Katul, G., C.-I. Hsieh, D. Bowling, K. Clark, N. Shurpali, A. Turnipseed, J. Albertson, K. Tu, D. Hollinger, B. Evans, B. Offerle, D. Anderson, D. Ellsworth, C. Vogel, and R. Oren, 1999: Spatial variability of turbulent fluxes in the roughness sublayer of an even-aged pine forest. *Bound.-Layer Meteorol.*, **93**, 1–28.

20. Loescher, H., T. Ocheltree, B. Tanner, E. Swiatek, B. Dano, J. Wong, G. Zimmerman, J. Campbell, C. Stock, L. Jacobsen, Y. Shiga, J. Kollas, J. Liburdy, and B. Law, 2005: Comparison of temperature and wind statistics in contrasting environments among different sonic anemometer-thermometers. *Agric. Forest Meteorol.*, **133**, 119–139.

21. Meijninger, W., 2003: *Surface fluxes over natural landscapes using scintillometry*. Ph.D. thesis, Wageningen University, Wageningen, The Netherlands.

22. Meijninger, W. and H. de Bruin, 2000: The sensible heat flux over irrigated areas in western turkey determined with a large aperture scintillometer. *J. Hyrdol.*, **229**, 42–49.

23. Meijninger, W., O. Hartogensis, W. Kohsiek, J. Hoedjes, R. Zuurbier, and H. de Bruin, 2002: Determination of area averaged sensible heat fluxes with a large aperture scintillometer over a heterogeneous surface - flevoland field experiment. *Bound.-Layer Meteorol.*, **105**, 63–83.

24. Moene, A., W. Meijninger, O. Hartogensis, B. Heusinkveld, and H. de Bruin, 2005: The effect of finite accuracy in the manufacturing of large aperture scintillometers. *Internal Report 2005/1, Meteorology and Air Quality Group, Wageningen University, Wageningen, the Netherlands*, 99 pp.

25. Nakaya, K., C. Suzuki, T. Kobayashi, H. Ikeda, and S. Yasuike, 2007: Spatial averaging effect on local flux measurement using a displaced-beam small aperture scintillometer above the forest canopy. *Agric. Forest Meteorol.*, **145**, 97–109.

26. Panofsky, H. and J. Dutton, 1984: *Atmospheric Turbulence*. John Wiley & Sons, New York, 397 pp.

27. Poggio, L., M. Furger, A. Prevot, W. Graber, and E. Andreas, 2000: Scintillometer wind measurements over complex terrain. *J. Atmos. Ocean Tech.*, **17(1)**, 17–26.

28. Schüttemeyer, D., 2005: *The surface energy balance over drying semi-arid terrain in West Africa*. Ph.D. thesis, Wageningen University, Wageningen, The Netherlands.

29. Wesely, M., 1976: The combined effect of temperature and humidity on the refractive index. *J. Appl. Meteorol.*, **15**, 43–49.

30. Wilson, K., A. Goldstein, E. Falge, M. Aubinet, D. Baldocchi, P. Berbigier, C. Bernhofer, R. Ceulemans, H. Dolmanh, C. Field, A. Grelle, A. Ibrom, B. Lawl, A. Kowalski, T. Meyers, J. Moncrieff, R. Monsonn, W. Oechel, J. Tenhunen, R. Valentini, and S. Verma, 2002: Energy balance closure at FLUXNET sites. *Agric. For. Meteorol.*, **113**, 223–243.

31. Wyngaard, J., Y. Izumi, and S. C. Jr., 1971: Behavior of the refractive-index-structure parameter near the ground. *J. Opt. Soc. Amer.*, **61**, 1646–1650.